

Improvements in the NIST Johnson Noise Thermometry System

Samuel P. Benz, *Senior Member, IEEE*, Jifeng Qu, Horst Rogalla, *Member, IEEE*, D. Rod White, *Member, IEEE*, Paul D. Dresselhaus, Weston L. Tew, *Member, IEEE*, and Sae Woo Nam

Abstract—We have developed a Johnson noise thermometry (JNT) system that is calibrated by precision waveforms synthesized with a quantized voltage noise source (QVNS). Improvements to the QVNS and the cross-correlation measurement electronics have significantly reduced systematic errors and measurement uncertainty. We describe in detail a number of these improvements, such as amplifier performance and frequency response. We also show details of recent measurements that characterize the nonlinearities and distortion properties of the measurement electronics. Finally, we present an uncertainty analysis and discuss the potential for the QVNS-JNT technique to contribute to the redefinition of Boltzmann's constant.

Index Terms—Boltzmann's equation, correlation, digital-analog conversion, Josephson arrays, measurement units, noise measurement, quantization, signal synthesis, standards, temperature.

I. INTRODUCTION

JOHNSON noise thermometry (JNT) is a primary thermometry technique that is based on the Johnson–Nyquist noise of a resistor, for which the mean-square voltage is proportional to Boltzmann's constant k , the temperature T , the resistance R , and the measurement bandwidth Δf : $\langle V^2 \rangle = 4kTR\Delta f$ [1]–[3]. Because the relation is fundamental, JNT is one of the few techniques that can determine absolute (thermodynamic) temperatures. The main challenge of JNT is that it requires accurate low-noise correlation techniques to measure the extremely small ~ 1.2 nV/Hz^{1/2} noise voltage of a typical 100 Ω resistor at the triple point of water ($T_{\text{tpw}} \equiv 273.16$ K).

The unique aspect of the National Institute of Standards and Technology (NIST) JNT system is that the electronics are calibrated with quantum-accurate pseudo-noise voltage waveforms, which are generated by a superconducting quantized voltage noise source (QVNS) made from Josephson junction arrays [4]–[8]. Since the start of NIST's JNT program in 2000, our goal has been to improve thermodynamic temperature

measurements. This has been accomplished primarily through ratio measurements that compared the electrical noise synthesized by the QVNS source and the thermal noise generated by resistors at various reference temperatures [8], [9]. To date, the most important contribution produced by the QVNS-JNT system has been a better understanding of the deviations of the International Temperature Scale of 1990 (ITS-90) from thermodynamic temperature. In particular, measurements have been performed at the moderately high temperatures of the zinc (692.677 K) and tin (505.078 K) freezing points [9]. The JNT results agreed with those from archival gas thermometry and radiation thermometry, providing an important independent method for determining thermodynamic temperature [10].

The QVNS-JNT system has also been used to measure lower temperatures, such as the water and gallium (302.9166 K) triple points. However, our previous best measurement at the water triple point was limited by systematic errors, which resulted in a 165 $\mu\text{K/K}$ (45 mK) disagreement with the SI value [7]. Similarly, the Ga triple point temperature disagreed by 150 $\mu\text{K/K}$ (46 mK) from the ITS-90 value. The temperatures similarly disagreed, so a good agreement occurred for the ratio of the two temperatures.

With the improvements that are described in this and two other papers [11], [12], we have reduced these dominant systematic errors and the measurement uncertainties so that absolute (in contrast to ratio and relative [5], [7]) temperature measurements can practically be performed for the first time. We can now consider using the QVNS-JNT system as an “Electronic kelvin” that links the SI kelvin to quantum-based electrical measurements. The system is particularly interesting as an electronic determination of Boltzmann's constant. The current relative standard uncertainty of Boltzmann's constant is 1.8×10^{-6} , which is predominately determined from a single measurement of the molar gas constant by another primary method: acoustic-gas thermometry [13]–[16]. Moldover *et al.* used this method in 1986 to measure the speed of sound in argon and achieved the lowest uncertainty to date of 1.7×10^{-6} [13]. Another gas thermometry approach that measures a gas's dielectric constant with audio-frequency capacitance bridges has achieved an uncertainty of 15×10^{-6} [17].

The NIST QVNS-JNT system offers an electronic approach, which is distinctly different from the gas-thermometry methods, and has the potential to significantly contribute to a new determination of Boltzmann's constant, provided that the total measurement uncertainty can be reduced below 1×10^{-5} . Because the QVNS-JNT system matches the electrical power and the thermal noise power at the triple point of water, which

Manuscript received June 6, 2008; revised August 15, 2008. First published November 21, 2008; current version published March 10, 2009. This work was supported by the National Institute for Standards and Technology. The Associate Editor coordinating the review process for this paper was Dr. Yi-hua Tang.

S. P. Benz, J. Qu, P. D. Dresselhaus, and S. W. Nam are with the National Institute of Standards and Technology, Boulder, CO 80305 USA (e-mail: samuel.benz@nist.gov).

H. Rogalla is with the Department of Applied Physics, University of Twente, 7500 Enschede, The Netherlands.

D. R. White is with the Measurement Standards Laboratory, Lower Hutt, 5040, New Zealand.

W. L. Tew is with the National Institute of Standards and Technology, Gaithersburg, MD 20899 USA.

Digital Object Identifier 10.1109/TIM.2008.2007027

U.S. Government work not protected by U.S. copyright.

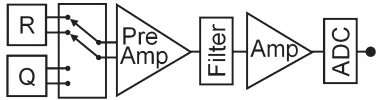


Fig. 1. Component schematic for a single channel of the JNT electronics. All components from the resistor (R) and QVNS (Q) signal sources up to the second amplifier have been improved, including the differential transmission lines to the differential preamplifier (shown as paired wires).

is the defining temperature for the SI kelvin, the measurements determine the ratio of the Boltzmann and Planck constants k/h . Since the 5×10^{-8} relative standard uncertainty of Planck's constant is much lower than that of k , any determination of k/h at the $\sim 10^{-6}$ level essentially determines k at that same uncertainty [14]. As described in Section VII, our present uncertainty in k/h is about 25×10^{-6} , and we hope to achieve a total combined uncertainty of 6×10^{-6} with further improvements.

II. QVNS-JNT SYNTHESIS AND MEASUREMENT TECHNIQUE

The QVNS uses precision waveform synthesis techniques that were developed for the AC Josephson Voltage Standard [4], [6], [18]. However, the lower voltages and longer integration times required for noise thermometry require a specialized QVNS circuit design that consists of a symmetric pair of grounded lumped arrays only having a small total number of junctions (typically $N_J = 8-256$). Each array is separately biased with a unipolar pulse drive that is clocked at the 10 GHz sampling frequency f_s . The accuracy of the QVNS waveforms is made possible by the perfect quantization of the output voltage pulses that are integer multiples of the inverse Josephson constant $K_J^{-1} \equiv h/2e$, where e is the electron charge. The synthesized waveform has a minimum frequency called the pattern repetition frequency $f_1 = f_s/M$ that is determined by the clock frequency and the bit length M of the digital waveform.

Pseudo-noise waveforms are constructed by summing equal-amplitude random-phase harmonics of this pattern repetition frequency. The RMS voltage amplitude V of each tone is chosen so that the synthesized waveform's average power spectral density $S_Q = \langle V^2 \rangle / f_1$ matches the thermal noise power spectral density $S_R = 4kRT$ to within 0.05%. The power spectral density of the calculable pseudo-noise waveform $S_Q = D^2 N_J^2 f_s M / K_J^2$ is represented by fundamental constants and integers, except for the clock frequency and the dimensionless factor D that appropriately scales the voltage and is calculable from the digital code sequence [6], [18].

The cross-correlation measurement electronics consists of two nominally identical channels. The schematic of one channel is shown in Fig. 1. The resistor and QVNS-synthesized voltage signals are alternately amplified and filtered, depending on the position of the switching network. The analog-to-digital converter (ADC) electronics samples these signals for 1 s with a 2.08 MHz sampling frequency. This produces frequency resolution bins of 1 Hz and, as shown in Fig. 2, a 1.04 MHz Nyquist frequency (f_N), above which the sampled frequencies are aliased back into this measurement bandwidth. The complex

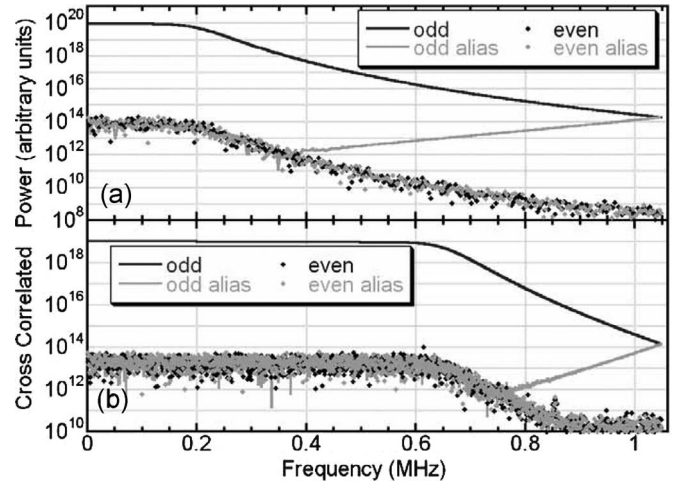


Fig. 2. Measured FFT cross-correlation spectra of QVNS-synthesized pseudo-noise waveforms with only odd-harmonic tones using the (a) “2006” (digitally filtered, 1.6 kHz spaced 1 Hz bins, 128 junctions) and (b) “2007” (passively filtered, 400 Hz spaced bins, eight junctions) circuits.

frequency-domain autocorrelation signals of each (A and B) channel are the average of 100 fast Fourier transform (FFT) spectra that are calculated from the 1 s long sampled intervals. The measured signals from both channels are then cross correlated in software to remove the uncorrelated noise from each channel. The switching network alternately switches the circuit to measure the different sources.

The cross-correlated electrical and thermal noise powers are compared over discrete bandwidths centered at each harmonic tone such that the bandwidth corresponds to the tone spacing of the synthesized waveform, which is typically f_1 for all-harmonic tones and $2f_1$ for odd or even tones. The ratio of the measured spectral densities $\langle S_R/S_Q \rangle$ at each frequency is of order unity and can be used to estimate the absolute temperature

$$T(f) = \left(\frac{\langle S_R \rangle}{\langle S_Q \rangle} \right)_f \frac{D^2 N_J^2 f_s M}{4k X_R R_K K_J^2} \quad (1)$$

where the resistance is expressed as the ratio X_R in units of the von Klitzing resistance $R_K \equiv h/e^2$ [13]. Equation (1) is a realization of an “Electronic kelvin” and is the basis of our QVNS-JNT technique in the absolute measurement mode [4]–[7].

Figs. 3 and 4 show plots of the ratio $\langle S_R \rangle / \langle S_Q \rangle$ as a function of frequency for different QVNS-JNT circuits that were used over the past four years. All plots clearly show a significant frequency dependence of the ratio, although the frequency dependence decreases for the most recent circuits. The noise power ratio should be close to unity so that deviations from unity indicate that the measured power spectral densities of the resistor and synthesized noise waveforms are unmatched. Over the eight-year-long NIST JNT program, we have uncovered the causes of the frequency-dependent mismatch, and we describe them in the following section along with the improvements that have reduced the systematic errors and uncertainty and have allowed the first practical measurements of absolute temperature.

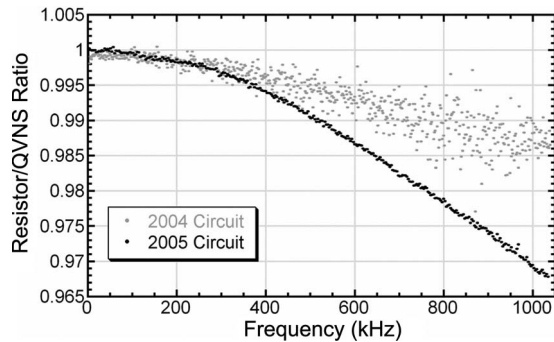


Fig. 3. Ratios of the measured cross-correlated power of the resistor Johnson noise and the QVNS pseudo-noise waveform comparing the frequency response of the 2004 and 2005 circuits.

III. IMPROVEMENTS

In our earliest measurements, the most important source of systematic errors arose from the distortion that is generated by various wires and wiring connections throughout the measurement circuit and electronics. This distortion produced the scatter in the ratio data for the 2004 circuit shown in Fig. 3. We found that the scatter, which increases with increasing frequency, was related to the distortion in either channel and in the transmission lines connecting the resistor and QVNS signals to the switchboard. The specific sources were found through careful autocorrelation and cross-correlation measurements of the QVNS-synthesized tones: typically odd-harmonic waveforms. The culprits that caused these nonlinearities were oxidized solder and gold-gold contact connections, kinked wires, and even some multifilament wires. All were found to behave nonlinearly and produce distortion in spite of the fact that they had low dc resistance. Directly soldering the superconducting circuits to the microwave packaging (instead of using wire-bonded or gold spring finger connections) also reduced the distortion.

These nonlinear features having been removed, the 2005 circuit data in Fig. 3 produced a scatter-free power ratio. However, these data still have a large frequency dependence, which is due to the different transmission lines and output impedance for the resistor and QVNS circuits [11]. Since the QVNS source behaves as a true voltage source, the differential output resistances of each QVNS differential-lead pair must be double that of the resistance ($2R$). The frequency response of the resistor and QVNS transmission lines was further tuned by adding lumped resistive, inductive, or capacitive components to the appropriate transmission lines. The resulting improvement from transmission line and impedance matching produced the flatter frequency response of the 2006 circuit data shown in Fig. 4. All of the above improvements contributed to lower uncertainty and better agreement for measurements of the 2006 circuits and for the high-temperature comparisons [9].

After matching the frequency response of the resistor and QVNS sources, we were able to characterize and improve other frequency-dependent effects caused by aliasing, filters, and numerical integration of the measured spectra [11], [12]. For example, the use of a bit stream generator with larger memory allowed us to produce waveforms with four-times finer tone

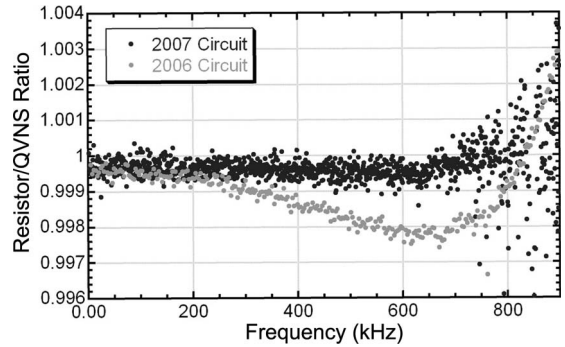


Fig. 4. Ratios of the measured cross-correlated power of the resistor Johnson noise and the QVNS pseudo-noise waveform comparing the frequency response of the 2006 and 2007 circuits.

spacing (400 Hz versus 1.6 kHz), which is used in the 2007 circuit data shown in Figs. 2(b) and 4. Finer tone spacing allows better matching near the cutoff frequencies of the filters.

The most significant improvement in the 2007 circuit is a new preamplifier design that has about 40 dB better common-mode rejection at 100 kHz (100 dB CMR) and 0.72 times lower noise compared to the previous preamplifier's $1.9 \text{ nV/Hz}^{1/2}$ noise floor. Our total measurement bandwidth was also improved by replacing the 150 kHz four-pole digital filter (that followed the ADC in Fig. 1) with a 650 kHz cutoff-frequency 11-pole passive filter (shown between the amplifier stages). This higher cutoff frequency and faster rolloff increased the measurement bandwidth and reduced the impact of aliased signals adding into the low-frequency noise power.

IV. ABSOLUTE TEMPERATURE MEASUREMENTS

Figs. 2 and 4 compare our best measurements of the 2006 and 2007 circuits. The 2007 circuit uses the improved amplifier, the passive filter, and the finer QVNS tone spacing. The different frequency response for these two circuits, due to the different filtering, is shown in Fig. 2. We only plot the odd and even bins of the measured FFT spectra. Both synthesized waveforms contained only odd-harmonic tones. Bins containing aliased tones, which are produced by tones above 1.04 MHz, are shown in grey. The odd tones map the transfer function of the respective circuits, whereas the even bins show the noise floor and undesirable distortion signals.

The 2006 circuit data in Fig. 2(a) show no even distortion harmonics above the noise floor, whereas the 2007 circuit data in Fig. 2(b) show a large even tone near 630 kHz, and others above 900 kHz. These "distortion" tones indicate the presence of unwanted nonlinearities in the passive filter or in the electronics' response to the filter. Since we only use the data below 600 kHz, these errors do not affect the temperature measurement.

Fig. 4 shows the ratio of cross-correlated power spectra for the resistor and QVNS as measured by the two different circuits. The frequency dependence is quite small for both ratios as a result of the matched transmission lines. Both circuits produce a reasonably linear frequency response up to the cutoff frequency of their filters. The remaining frequency dependence results from small differences between the QVNS and the

resistor transmission lines. For all of these ratio measurements, a quadratic fit was used to determine the temperature and remove any remaining frequency-dependent differences between the electronic and thermal power spectral densities [9], which result from small differences in the time constants due to imperfect impedance matching.

The signals from the 2006 circuit were integrated over 36 h to achieve a Type A $1\text{-}\sigma$ uncertainty of $42\ \mu\text{K/K}$ (11.5 mK) over a 150 kHz bandwidth. The indicated temperature is consistent with the SI-assigned temperature for the water triple point, yielding a relative temperature difference of $-28\ \mu\text{K/K}$ ($-7.6\ \text{mK}$). The 2007 circuit achieved a $19\ \mu\text{K/K}$ (5.2 mK) statistical uncertainty in the same 36 h over a 600 kHz bandwidth. Most importantly, these measurements indicated an agreement of $3 \pm 25\ \mu\text{K/K}$ ($0.8 \pm 6.8\ \text{mK}$) (including type B uncertainties) between the noise temperature and the SI temperature. The lower noise amplifier and the higher cutoff frequency filters of the 2007 circuit allow a wider bandwidth measurement and, thus, a faster integration time for a given uncertainty. By increasing the integration time to 20 days, this 2007 circuit configuration could achieve a $5\ \mu\text{K/K}$ (1.4 mK) uncertainty, which is more than an order of magnitude smaller than the uncertainty achieved in other noise thermometry measurements with comparable integration time.

V. NONLINEAR ELECTRONICS AND FREQUENCY RESPONSE

For many years, we have intentionally used pseudo-noise waveforms that only contained odd-harmonic tones. We chose not to use all-harmonic and even-harmonic tones because measurements of the resistor–QVNS power ratio using these waveforms contained randomly scattered values that are uniformly distributed with frequency. Further integration of these data did not reduce the scatter and, therefore, the measurement uncertainty, as one would expect if the measurement were dominated by uncorrelated white noise. When odd harmonics were used, however, the scatter vanished, and the measurement uncertainty continued to decrease with integration time, as expected. This indicated that the electronics were generating much more even-harmonic distortion than odd-harmonic distortion, because even-harmonic distortion does not significantly contribute to the RMS power when odd tones are used, but it does for patterns with even-harmonic and all-harmonic tones. Unfortunately, the even distortion was sufficiently small (less than $-60\ \text{dBc}$, more than 60 dB below the carrier or fundamental) that it was hidden below the cross-correlated noise floor.

Having significantly improved the measurement electronics, we are now attempting to better understand its intrinsic nonlinearities. Since the distortion is buried below both the amplifier and the cross-correlated noise floors for odd-harmonic pseudo-noise waveforms with large numbers of small amplitude tones, we used two-tone waveforms with larger amplitude tones to uncover the distortion. The new amplifiers are currently being analyzed in detail by use of the AC Josephson Voltage Standard system [19].

Preliminary measurements of two-tone waveforms synthesized with the QVNS have also revealed some of the distortion.

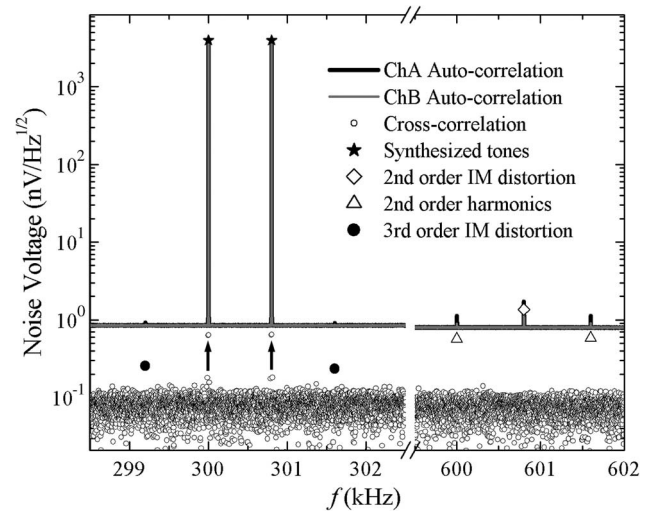


Fig. 5. Autocorrelation and cross-correlation measurements of the power spectral density of a QVNS-synthesized two-tone waveform. Second- and third-order intermodulation distortions and second-order harmonics are indicated with different symbols. The arrows point to pairs of 1 Hz bins (adjacent to each fundamental tone) that indicate the presence of phase noise from either the QVNS source or ADC measurement clocks. (Note that the y -axis units are in volts.)

In Fig. 5, we show the autocorrelation and cross-correlation measurements of a synthesized waveform having two tones (300 and 300.8 kHz) with $4\ \mu\text{V}$ rms amplitudes and zero relative phase. The distortion products are highlighted with different symbols. This plot emphasizes the difficulties in measuring such nonlinearities. The nonlinearities are practically invisible in the autocorrelated data (just a pixel or two above the noise floor). Cross correlating the signal reveals the presence of distortion. Unfortunately, since the nonlinearities in each channel are not necessarily the same, the cross-correlated data do not give useful quantitative distortion data for the individual channels. However, it does show that the second-order distortion is larger than the third-order distortion, as expected [11]. Further measurements are underway to characterize the amplitude and frequency response of the distortion.

Through these two-tone measurements, we have also found that different components in each channel have different amounts of even and odd distortion. In fact, the measurements uncovered a large second-order nonlinearity in an active anti-alias filter, which has a 2 MHz cutoff frequency and was used in all the 2007 and prior measurement circuits. After removing these active amplification components, the even-harmonic distortion was reduced. The large nonlinearity was probably due to a damaged component.

Through further measurements, we hope to reveal and reduce other significant sources of distortion. However, all the electronic components have a nonlinear response, with typical distortion ratings of the high-performance audio-frequency components being $-100\ \text{dBc}$ at 1 kHz (100 dB below the signal amplitudes, which is comparable to 0.0003% of the voltage for total harmonic distortion). For the distortion signals to contribute less than $1\ \mu\text{V/V}$ to a desired signal residing in the same frequency bin, they must be at least $-120\ \text{dBc}$. It is unlikely, if not impossible, that we can find better op-amps, FETs, and other components with such performance, particularly over a

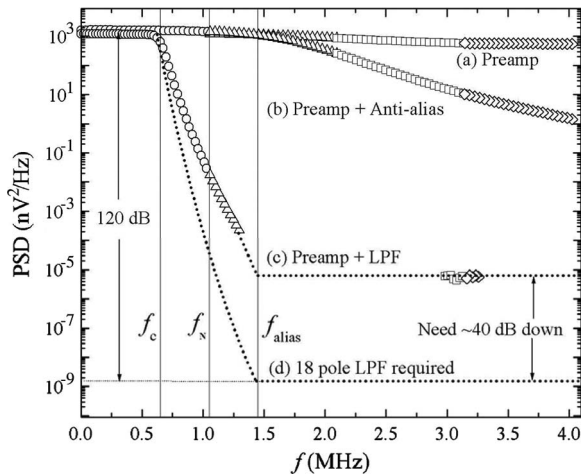


Fig. 6. (a)–(c) Transfer functions reconstructed from multiple alias harmonics for three different circuit configurations. Triangles, squares, and diamonds represent higher order aliased tones. (d) The fourth plot of dotted lines indicates the transfer function needed to ensure that no aliased signals affect the measurements of the noise power below 650 kHz. (Note that the y -axis units are in square volts.)

1 MHz bandwidth. Therefore, just as we have matched the power spectral density and frequency response for the thermal and electrical signals, we must now ensure that the noise power measured for our QVNS-synthesized waveforms reproduces the same nonlinearities produced by the thermal noise. Future QVNS waveforms will likely contain all the harmonic tones, and multiple pattern realizations that have different random phases will better resemble the white noise.

After removing the 2 MHz anti-alias filter with the large second-harmonic distortion, we observed that the passive 11-pole low-pass filter (LPF) has a -80 dBc stopband attenuation. Fig. 6 shows the measured transfer functions for three of the circuit configurations that include the new preamplifier. Although the ADC samples at 2 MHz, we can reconstruct the circuit transfer functions from multiple aliases of the QVNS tones, which were synthesized up to 4 MHz. Fig. 6(c) shows not only the faster rolloff of the passive filter but also the -80 dBc aliased signals of the stopband at around 3 MHz. A dotted line shows the expected transfer function and stopband level that was hidden by amplifier noise. As discussed for the nonlinearities in the previous paragraphs, these stopband signals must also be at least -120 dBc (40 dB lower) so that their aliased signals do not contribute to measurement of the desired noise signals. In addition, we need a higher order filter (at least 18 poles), as shown in Fig. 6(d), so that the signals at and above 1.43 MHz (above f_{alias}), when aliased below the cutoff frequency (f_c), also do not contribute to the measured power. To ensure the desired stopband, a second passive filter and another amplifier will be added before the ADC. We hope to include all of the above additional improvements in a “near-term” 2008 circuit.

VI. DETERMINATION OF BOLTZMANN’S CONSTANT

As discussed in Section I, thermodynamic temperature can now be directly measured with the QVNS-JNT system by measuring the absolute noise power. When the noise power

TABLE I
UNCERTAINTY BUDGET FOR THE RATIO OF THERMAL AND ELECTRICAL NOISE POWER SPECTRAL DENSITIES $\langle S_R \rangle / \langle S_Q \rangle$

Error Source	Relative Uncertainties (parts in 10^6)	
	2007	Near-Term
Statistics	19.0	5.2
Spectral Shape	5.0	1.0
Distortion	5.0	1.0
EMI	10.0	2.0
Root Sum Square Total	22.6	5.8

TABLE II
UNCERTAINTY BUDGET FOR THE k/h RATIO

Error Source	Relative Uncertainties (parts in 10^6)	
	2007	Near-Term
Noise Power Ratio	22.6	5.8
QVNS Errors	0.1	0.1
Sampling Frequency, f_s	0.001	0.001
Temperature, T	1.9	0.68
Resistance, X_R	10	1.1
Root Sum Square Total	24.8	5.9

comparison is made between the QVNS and a resistor at the water triple point, Boltzmann’s constant can be determined through the ratio

$$\frac{k}{h} = \frac{\langle S_R \rangle}{\langle S_Q \rangle} \frac{D^2 N_J^2 f_s M}{16 T X_R} \quad (2)$$

where $T = T_{\text{tpw}}$. In this paper, the conventional values K_{J-90} and R_{K-90} are sufficiently close to $K_J \equiv 2e/h$ and $R_K \equiv h/e^2$ that they can be used without correction [14]. Having reduced the systematic errors as described in the previous sections, the total measurement uncertainties of both the temperature (1) and Boltzmann’s constant (2) are now dominated by the measurement uncertainty of the ratio of power spectral densities $\langle S_R \rangle / \langle S_Q \rangle$.

The uncertainty budget for the ratio of the thermal and electrical noise power spectral densities is shown in Table I. The total root-sum-square uncertainty for the power density ratio is currently 23×10^{-6} and includes uncertainty contributions from the spectral shape (frequency response), distortion, and electromagnetic interference (EMI). However, the total uncertainty is dominated by the 19×10^{-6} statistical measurement uncertainty. In the near term, we intend to reduce the statistical uncertainty fourfold to around 5×10^{-6} by increasing the measurement time from 36 h to ten days and constructing a four-channel system that simultaneously measures both sources. The uncertainties of the other components can also be reduced through the aforementioned improvements and through additional measurements so that the total combined uncertainty for the measured power density ratios will be less than 6×10^{-6} .

As previously mentioned, the uncertainty budget for Boltzmann’s constant (equivalent to that for k/h) is also dominated by the statistical uncertainty (through the uncertainty in the noise power ratio), as indicated in Table II. Currently, our resistance uncertainty is also a significant contribution, and we plan to reduce it tenfold to 1.1×10^{-6} through improvements

in resistor stability and systematic routine calibrations carried out during the noise measurements. All of the “near-term” uncertainties are target values that we expect to reach in the next version of the QVNS-JNT system.

VII. CONCLUSION

Precision waveform synthesis with the QVNS has allowed us to significantly improve the JNT measurements. We have shown that the QVNS-synthesized waveforms are a powerful tool for characterizing the electronic nonlinearity and the frequency response of amplifiers, filters, and other components, as well as for providing an accurate quantum-based electronic reference. As a result of this capability and other improvements to the measurement electronics, absolute thermodynamic temperature measurements are now possible, so that the QVNS-JNT system can be considered to be an “Electronic kelvin.” We are optimistic that additional improvements and measurements will allow a practical “electronic” noise measurement of Boltzmann’s constant at a measurement uncertainty of 6×10^{-6} .

ACKNOWLEDGMENT

The authors would like to thank C. Burroughs for chip packaging, R. Toonen for helpful conversations regarding amplifier nonlinearities, T. Veening for electronics assembly, N. Bergren for QVNS fabrication, D. Ripple for helpful suggestions, and J. Martinis for inspiring the QVNS-JNT program and for designing the original electronics. A summary version of this paper is included in the CPEM 2008 Proceedings [20]. The work for paper was performed at NIST.

REFERENCES

- [1] J. B. Johnson, “Thermal agitation of electricity in conductors,” *Nature*, vol. 119, pp. 50–51, Jan. 1927.
- [2] H. Nyquist, “Thermal agitation of electric charge in conductors,” *Phys. Rev.*, vol. 32, no. 1, pp. 110–113, Jul. 1928.
- [3] D. R. White, R. Galleano, A. Actis, H. Brixy, M. De Groot, J. Dubbeldam, A. L. Reesink, F. Edler, H. Sakurai, R. L. Shepard, and J. C. Gallop, “The status of Johnson noise thermometry,” *Metrologia*, vol. 33, no. 4, pp. 325–335, Aug. 1996.
- [4] S. P. Benz, J. M. Martinis, S. W. Nam, W. L. Tew, and D. R. White, “A new approach to Johnson noise thermometry using a Josephson quantized voltage source for calibration,” in *Proc. TEMPMEKO, 8th Int. Symp. Temperature Thermal Meas. Ind. Sci.*, B. Fellmuth, J. Seidel, and G. Scholz, Eds., Berlin, Germany: VDE Verlag, 2001, pp. 37–44.
- [5] S. W. Nam, S. P. Benz, P. D. Dresselhaus, W. L. Tew, D. R. White, and J. M. Martinis, “Johnson noise thermometry measurements using a quantum voltage noise source for calibration,” *IEEE Trans. Instrum. Meas.*, vol. 52, no. 2, pp. 550–553, Apr. 2003.
- [6] S. P. Benz, P. D. Dresselhaus, and J. M. Martinis, “An AC Josephson source for Johnson noise thermometry,” *IEEE Trans. Instrum. Meas.*, vol. 52, no. 2, pp. 545–549, Apr. 2003.
- [7] S. W. Nam, S. P. Benz, P. D. Dresselhaus, C. J. Burroughs, W. L. Tew, D. R. White, and J. M. Martinis, “Progress on Johnson noise thermometry using a quantum voltage noise source for calibration,” *IEEE Trans. Instrum. Meas.*, vol. 54, no. 2, pp. 653–657, Apr. 2005.
- [8] S. W. Nam, S. P. Benz, J. M. Martinis, P. Dresselhaus, W. L. Tew, and D. R. White, “A radiometric method for Johnson noise thermometry using a quantized voltage noise source,” in *Temperature: Its Measurement and Control in Science and Industry*, vol. VII, D. C. Ripple, Ed. Melville, NY: AIP, 2003, pp. 37–42.
- [9] J. R. Labenski, W. L. Tew, S. W. Nam, S. P. Benz, P. D. Dresselhaus, and C. J. Burroughs, “A determination of the ratio of the zinc freezing point to the tin freezing point by noise thermometry,” in *Proc. TEMPMEKO 2007, Int. J. Thermophys.*, vol. 29, no. 1, Feb. 2008, pp. 1–17.
- [10] J. Fischer *et al.*, “Working Group 4 report to the CCT,” in *Consultative Committee for Thermometry, CCT/08-13*. Sevres, France: BIPM, 2008.
- [11] D. R. White and S. P. Benz, “Constraints on a synthetic-noise source for Johnson noise thermometry,” *Metrologia*, vol. 45, no. 1, pp. 93–101, Jan. 2008.
- [12] D. R. White, S. P. Benz, J. R. Labenski, S. W. Nam, J. F. Qu, H. Rogalla, and W. L. Tew, “Measurement time and statistics for a noise thermometer with a synthetic-noise reference,” *Metrologia*, vol. 45, no. 4, pp. 395–405, Jul. 2008.
- [13] M. R. Moldover, J. P. M. Trusler, T. J. Edwards, J. B. Mehl, and R. S. Davis, “Measurement of the universal gas constant R using a spherical acoustic resonator,” *J. Res. Nat. Bur. Stand. (U.S.)*, vol. 93, no. 3, pp. 88–144, Mar. 1988.
- [14] P. J. Mohr, B. N. Taylor, and D. B. Newell, “CODATA recommended values of the fundamental physical constants: 2006,” *Rev. Mod. Phys.*, vol. 80, no. 2, pp. 633–730, Apr.–Jun. 2008.
- [15] J. Fischer and B. Fellmuth, “Temperature metrology,” *Rep. Prog. Phys.*, vol. 68, no. 5, pp. 1043–1094, Mar. 2005.
- [16] J. Fischer *et al.*, “Preparative steps towards the new definition of the kelvin in terms of the Boltzmann constant,” *Int. J. Thermophys.*, vol. 28, no. 6, pp. 1753–1765, Dec. 2007.
- [17] B. Fellmuth, J. Fisher, C. Gaiser, N. Haft, “Dielectric-constant gas thermometry and determination of the Boltzmann constant,” in *Proc. TEMPMEKO, 9th Int. Symp. Temperature Thermal Meas. Ind. Sci.*, D. Zvizdić, L. G. Bermanec, T. Stašić, and T. Veliki, Eds., Zagreb, Croatia: LPM/FSB, 2004, vol. 2, pp. 73–78.
- [18] S. P. Benz and C. A. Hamilton, “A pulse-driven programmable Josephson voltage standard,” *Appl. Phys. Lett.*, vol. 68, no. 22, pp. 3171–3173, May 1996.
- [19] R. C. Toonen and S. P. Benz, “Nonlinear behavior of electronic components characterized with precision multitones from a Josephson arbitrary waveform synthesizer,” in *IEEE Trans. Appl. Supercond.*, Jun. 2009, to be published.
- [20] S. P. Benz, H. Rogalla, D. R. White, J. Qu, P. D. Dresselhaus, W. L. Tew, and S. W. Nam, “Improvements in the NIST Johnson noise thermometry system,” presented at the Conf. Precision Electromagnetic Measurements Dig., Broomfield, CO, Jun. 9–13, 2008, MA-2-1.



Samuel P. Benz (M’00–SM’00) was born in Dubuque, IA, on December 4, 1962. He received the B.A. degree (*summa cum laude*) in physics and math from Luther College, Decorah, IA, in 1985 and the M.A. and Ph.D. degrees in physics from Harvard University, Cambridge, MA, in 1987 and 1990, respectively.

Since 1990, he has been with the National Institute of Standards and Technology (NIST), Boulder, CO, where he was a NIST/NRC Postdoctoral Fellow and a permanent Staff Member in January 1992 and has been the Project Leader of the Quantum Voltage Project since October 1999. He has worked on a broad range of topics within the field of superconducting electronics, including Josephson junction array oscillators, single flux quantum logic, ac and dc Josephson voltage standards, and Josephson waveform synthesis. He has 150 publications and is the holder of three patents in the field of superconducting electronics.

Dr. Benz is a member of Phi Beta Kappa and Sigma Pi Sigma. He was the recipient of two U.S. Department of Commerce Gold Medals for Distinguished Achievement. He received an R. J. McElroy Fellowship (1985–1988) to work toward the Ph.D. degree.



Jifeng Qu was born in Xi’an, China, on December 16, 1978. He received the B.S. degree in materials physics and the Ph.D. degree in condensed matter physics from the University of Science and Technology of China, Hefei, China, in 2001 and 2006, respectively. His doctoral research focused on the charge stripe ordering in high-temperature superconducting cuprates.

Since April 2007, he has been with the National Institute of Standards and Technology (NIST), Boulder, CO, where he was previously a Guest Researcher and is currently working on the Johnson Noise Thermometry program and investigating electronic nonlinearities using superconducting quantum-based voltage sources.



Horst Rogalla (M'96) was born in 1947. He received the Ph.D. degree in physics from Westfälische Wilhelms-Universität Münster, Münster, Germany, in 1979.

In 1977, he was with the Faculty of Physics, Giessen, Germany, where he habilitated in 1986. Since 1987, he has been a Professor with the Department of Applied Physics, University of Twente, Enschede, The Netherlands, where he is also the Head of the Low-Temperature Division. He is active with the University Institutes for Nanotechnology

MESA+ for Sustainable Energy (IMPACT) and the Biomedical Technology Institute (BMT/TG). He also heads the European superconducting electronics network known as Fluxonics. His research interests are in superconducting electronics and materials science, particularly in relation to thin-film growth and properties.

Dr. Rogalla is a member of the Dutch, German, and American Physical Societies as well as the American and European Materials Research Society. He is also a member of the board of the European Society for Applied Superconductivity (ESAS), after being its President for many years.



D. Rod White (M'95) received the M.Sc. degree (First-Class Hons. in physics) from the University of Waikato, Hamilton, New Zealand, in 1980.

He is currently the Team Leader of the Temperature Section with the Measurement Standards Laboratory, Lower Hutt, New Zealand. His research interests span a broad range of temperature measurement topics and include Johnson noise thermometry, propagation of measurement uncertainty, calibration of resistance bridges, the triple point of water, and radiation thermometry. He is the author of more than

80 scientific papers, coauthor of the text *Traceable Temperatures*, and author of several contributions to texts and encyclopaedia.

Mr. White received the Silver Medal and the Cooper Medal from the New Zealand Royal Society for contributions to temperature metrology, and he is active with several of the working groups associated with the CIPM Consultative Committee on Thermometry (CCT).



Paul D. Dresselhaus was born in Arlington, MA, on January 5, 1963. He received the B.S. degree in physics and electrical engineering from the Massachusetts Institute of Technology, Cambridge, in 1985 and the Ph.D. degree in applied physics from Yale University, New Haven, CT, in 1991.

In 1999, he was with the Quantum Voltage Project, National Institute of Standards and Technology, Boulder, CO, where he has developed novel superconducting circuits and broadband bias electronics for precision voltage waveform synthesis and program-

mable voltage standard systems. He was with Northrop Grumman for three years, where he designed and tested numerous gigahertz-speed superconducting circuits, including code generators and analog-to-digital converters. He also upgraded the simulation and layout capabilities at Northrop Grumman to be among the world's best. He has also been a Postdoctoral Assistant with the State University of New York, Stony Brook, where he worked on the nanolithographic fabrication and study of Nb-AlO_x-Nb junctions for single-electron and SFQ applications, single-electron transistors and arrays in Al-AlO_x tunnel junctions, and the properties of ultrasmall Josephson junctions. He is currently with the National Institute of Standards and Technology, Boulder, CO.



Weston L. Tew (M'90) was born in Glen Cove, NY, in 1957. He received the B.S. degree in physics from Antioch University, Yellow Springs, OH, in 1980 and the Ph.D. degree in physics from the University of Colorado, Boulder, in 1989.

From 1980 to 1981, he was a Sensor Engineer with YSI, Inc., Yellow Springs. In 1989, he was an NRC Postdoctoral Associate with the Electricity Division, National Institute of Standards and Technology (NIST), Gaithersburg, MD, where he worked on dc current sources and the Watt balance. In 1992,

he was a Guest Scientist with the Mass Section, BIPM, Sevres, France, where he worked on anelastic relaxation in torsional suspensions. In 1993, he joined the Process Measurements Division, NIST, where he currently works on low-temperature thermometry, gas-based fixed points, and noise thermometry.

Dr. Tew is a member of the American Physical Society, the Instrumentation, Systems and Automation Society, and the American Society for Testing and Materials.



Sae Woo Nam received the degree in physics and electrical engineering from the Massachusetts Institute of Technology, Cambridge, in 1991 and the M.S. and Ph.D. degrees in physics from Stanford University, Stanford, CA, both in 1998. His thesis research focused on the development of large cryogenic detectors for the direct detection of dark matter particles using superconducting transition-edge sensors for the Cryogenic Dark Matter Search experiment (CDMS). As part of the CDMS experiment, he designed the TES readout

electronics for 168 independent channels.

While at Stanford University, he was involved with the first demonstration of using TES sensors to directly detect optical photons, as well as the first use of a TES optical photon sensor to look at an astronomical object. He is currently with the National Institute of Standards and Technology, Boulder, CO.